Investigation of ductile/brittle chip formation zone in the context of manufactured geometry with different CAM paths strategies

László Móricz*, Zsolt Viharos János**,***

* *University of Pannonia, Faculty of Engineering, Mechatronic Education and Research Institute, Zalaegerszeg, Hungary;(e-mail: moricz1888@gmail.com).*

* *Zalaegerszeg Center of Vocational Training, ZSZC Ganz Ábrahám Technical School*

** *Institute for Computer Science and Control (SZTAKI), Centre of Excellence in Production Informatics and Control, Center of Excellence of the Hungarian Academy of Sciences (HAS), Eötvös Loránd Research Network (ELKH), Budapest, Hungary, (e-mail: viharos.zsolt@sztaki.hu)*

*** *John von Neumann University, Kecskemét, Hungary, (e-mail: viharos.zsolt@gtk.uni-neumann.hu)*

Abstract: For maintenance conform processing of brittle materials (ceramics, glass), the resulting chips are not continuous, as in the case of soft and tough materials, it is called a brittle chip removal range. In this machining zone, the quality of the produced surface may decline (appears the cracks and pitting of the material) and the tool life also decreases. When defining the cutting technology (technological parameters, tool edges, tool cooling / lubrication, etc.), chip removal must be carried out in the ductile range. However, due to tool wear, this range may cross the transition and then it can work in the brittle chip formation zone. In this paper, the machinability of zirconia oxid ceramics has been investigated. The aim of the research is to find out the correlation between the wear of the cutting tool, the volume change of the manufactured pockets and the transitions between the chip formation ranges measured by cracks and pitting deformations on the edge of the machined material. It was observed that they overlap to a large extent, consequently, these observed phenomena can be easily applied for tool wear and quality monitoring for realising condition-based maintenance, it is the main scientific contribution of the paper.

Keywords Ductile/brittle chip formation zone, ceramics, micro-milling, indirect tool wearing monitoring.

1. INTRODUCTION

Manufacturing companies are currently facing high productivity and cost pressures (Bauernhansl, 2020), one of the key factors of the maintenance of the complete system and its components, e.g., machines, tools, measurement units, etc (Spath et al., 2017) (Glawar et al., 2021). Among various performance viewpoints, the machining time (and also the throughput time) and the machining tool lifetime is especially important. At material removal manufacturing, the delivery time and the production cost can be significantly reduced by increasing the cutting tool life. Longer tool life means reduced tool costs, and significant production time can be saved mainly for mass production by minimizing the number of tool replacements.

For tough materials (steels etc.), the possibilities for increasing the life of the cutting tool are mainly well defined, however, there are many unexplored areas for brittle materials (ceramics, glass etc.). An example is the behaviour of brittle materials in the cutting separation zone.

In the case of soft and tough materials (plastics, steels, etc.) the process of chip removal goes through the following phases: elastic deformation of the chip element in the deformation zone, plastic deformation of the chip element in the deformation zone, shear element shear along the shear plane.

In the case of brittle materials (ceramic, glass), the material is not able to flexibly follow the change in the cutting force, so the chip element bounces from the surface. The fundamental premise of ductile mode cutting states (DMC) that all brittle material will face a transition from DMC to Brittle Mode Cutting (BMC) when cutting from zero depth of cut (DoC) to a large value regardless its hardness and brittleness. When cutting below the critical undeformed chip thickness (UCT), the energy consumed for crack prorogation is larger than that for ductile deformation, DMC will be achieved in brittle materials successfully (Antwi et al., 2018).

When machining ceramics and other brittle materials, the key question for tool wear is whether the position of the working point can be moved between the ranges of brittle-ductile chip removal. There is a lot of published research on the topic where the authors are looking for the answer to this question. (Rong et al., 2018, and Muhammad et al., 2013). This topic was investigated by W. S. Blackley et al. (1991), who have worked on setting up a cutting model to turn the process into a ductile range when turning brittle material with diamond. Compared to the variables used in traditional cutting models, the article introduces two new variables: critical cutting depth (d_c), average crack depth (y_c). It is found that increasing the face angle in the negative direction improves productivity by

increasing the critical depth of cut within which the tool is still operating in the ductile chip removal range.

Muhammad Arif et al. (2012) investigated the evolution of the brittle-ductile chip separation region during the machining of WC-TaC-TiC composite. An analytical model is presented for how to create a crack-free surface by milling for brittle materials. The critical conditions of machining have been determined in the model, considering the radial depth of cut and the destructions under the machined surface that occur during cutting due to the brittle fracture of the chip elements. If the radial depth of cut is greater than the depth of subsurface decay of the machined material, crack-free machining is possible at the boundary of the ductile and brittle chip removal range. If the radial depth of cut is less than the depth of the cracks below the machined surface, brittle chip breakage can be prevented by milling in the ductile range to produce a crack-free surface. Furthermore, it was found that the feed rate per tooth together with the depth of cut determine the target range. It has been found that the depth of cut feed values have a critical value that affects the resulting chip removal process. Below a certain depth of cut, the feed rate can be greatly increased without chip formation in the brittle range.

The scientific literature recommends in the form of an approximate formula for determining an optimal depth of cut, in order to work in the range of ductile chip removal (Heleenet al. 2014, Rong et al. 2012, Rong et al. 2013). The relationship is given in the following form:

$$d_{crit} = 0.15 \left(\frac{E}{H}\right)\left(\frac{K_{Ic}}{H}\right)^2 \tag{1}$$

Where:
- E: Young modulus (GPa)
- H: hardness (kg/mm^2)
- K_{Ic}: fracture toughness (MPa m$^{1/2}$)

The empirical formula was developed by Bifano et al., 1991. For grinding brittle material, but also applies this relationship to ceramic milling. The literature (Heleenet al. 2014, Rong et al. 2012, Rong et al. 2013) also suggests another objective function to provide ductile chip separation, which can be used to determine the value of a recommended maximum chip thickness as a function of technological parameters. The relationship is given in the following form:

$$h_{max} = r_\varepsilon - \sqrt{r_\varepsilon^2 + f_z^2 - 2f_z\sqrt{2r_\varepsilon a_p - a_p^2}} \tag{2}$$

Where:
- h_{max}: maximum chip thickness (mm)
- r_ε: tool tip radius (mm)
- a_p: axial depth of cut (mm)
- f_z: feed per tooth (mm/fog)

Ueda et al. (1991) also tried to model the processes in the chip separation zone and to quantify the parameters that can be used to decide in which range the machining process is expected for a given material with a given technology. In their article, several raw materials (zirconium oxide, WC-Co, Al$_2$O$_3$, Si$_3$N$_4$,

SiC) were investigated, which led the authors to conclude that materials with high fracture toughness can be easily machined in the range of ductile chip removal at low depth of cut and high cutting speeds. At low fracture strength values, the ductile chip removal range could not be reached even with the small depth of cut used in the experiment. At low fracture toughness, no parameter combination was found to move the process into the range of ductile chip formation zone. Based on the research so far, it can be concluded that the breaking strength of the material, the applied feed rate, and the depth of cut have a decisive influence on the machining range. However, the angular position of the tool and the workpiece relative to each other also affects the machining range (Kevin et al. 2009). The research is mainly important during machining with a ball mill and torus mill, as it is here that we can talk about the effective cutting speed (cutting speed value depending on the axial depth of cut). A review of the literature shows that the optimal value of the tilt angle of the tool is to be found between 40 and 60° for the tested brittle material.

The purpose of this article is to determine the relationship between the change in volume calculated from the geometrical characteristics of each pocket produced and the chipping of the ceramics material resulting from the change in the ductile-brittle chip formation zone with each wear phase of the tool edge angle system.

2. EXPERIMENTAL CONDITIONS

The workpiece material used in the experiment is an oxide ceramics material applied by sintering to a carbide base. The machining tool is a TiAlN coated 1 [mm] diameter 2-edge ball end milling tool. The technological parameters used are the following: *speed, n [1 / min]: 25000; feed, v_f [mm / min]: 300; axial depth of depth, a_p [mm]: 300μm; radial depth of cut, a_e [mm]: 300μm.* Toolpaths used in the experiment: *waveform, trochoidal toolpath (cycloid path), chained toolpath.*

The basis of the experiments was the milling machine that was planned and built by the CncTeamZeg group. It is operated in Zalaegerszeg, Hungary. During its planning, the aim was to cut metal material but the preliminary calculations and tests on ceramic material removal proved that it is able to cut ceramic material as well.

3. EVALUATION OF MEASUREMENT RESULTS

3.1. Examined features

The first step in the analysis is to determine the wear abrasion phase transitions of the tool. This can be done **directly** (examining the tool under a microscope) and **indirectly** (examining the change in size of machined pockets) (Móricz et al. (2020 a,b), and Móricz et al (2021 a, b)). The determination of the tool wearing was started by an indirect method. The separated chip volume was calculated based on the geometrical characteristics *(width, length, depth)* of the resulted workpiece pockets measured after the application of each path strategy, and then these values were plotted on a graph. The other area examined was the edges of the finished pockets.
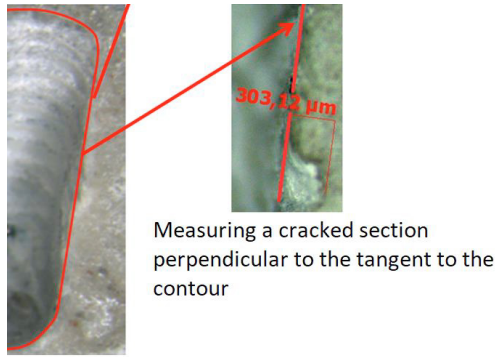
Figure 1. Examined characteristics of the manufactured pocket

During the evaluation, the outer edge of the pocket was examined (Fig. 1.). On the one hand, the cracking of the raw material after processing was measured, by the magnitude of the cracking of the material particles, and on the other hand, the number of occurrences of these defects along the circumference of the manufactured pockets were examined. During the evaluation, the 10 largest pitting were averaged, taking into account the length of the pitting and the depth in the vertical direction.
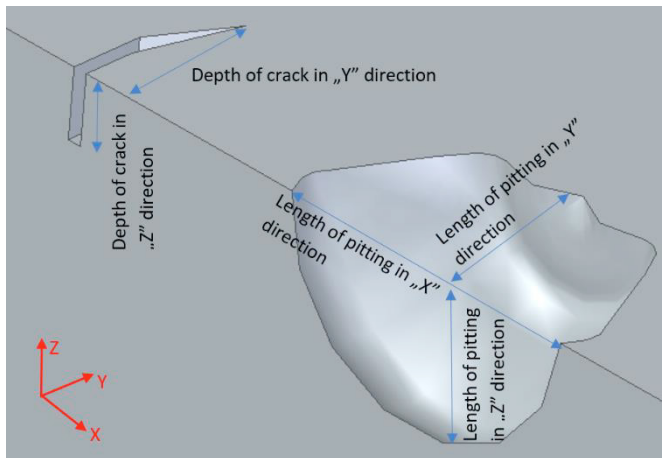
Figure 2. Geometric defects in manufactured pockets: The "y" direction of the cracks was taken into account during the quality test, while the "x-y-z" dimensions of the crack were taken into account in the case of cracking.

If the value of the pitting length (direction of "X") and the vertical depth (direction of "Z") was approximately twice to the horizontal depth of the error (direction of "Y"), the value of the largest of the 3 directions of the error was considered (Fig. 2.).

3.2. Set-up of the microscopy system

During the cutting process, microscopic images were taken repeatedly after a certain number of feature machining, in order to monitor in an offline way, the wearing evolution of the tool. Measurements were performed using Zeiss Discovery V8 microscope and the wearing in the pictures were evaluated by the authors. The tool was applied until its breakage, this served with the complete tool lifetime.

3.3. Results

It can be seen in Fig. 3, 4, 5 that the nature of the volume reduction in the pockets follows the Taylor curves (each pocket was measured in three directions once). A good distinction can be made between the wear phase worn-in, normal wear condition and the wear-out phase, even if it is partly a subjective evaluation, however, the changes in the curve progress for the different stages can be easily recognized. This can be most clearly observed in the waveform toolpath, but the wear phases can be well identified with the other technologies as well.
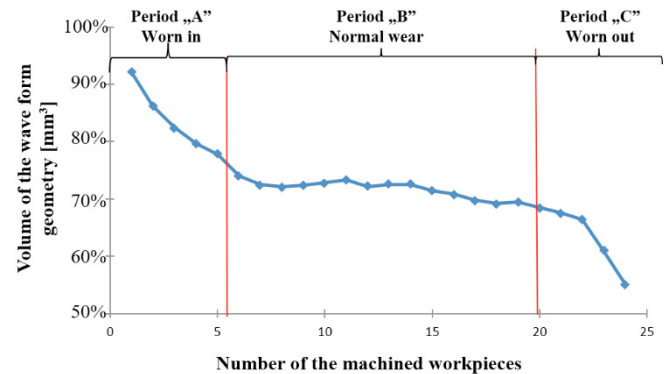

Figure 3. Changes in the volume of the machined pockets at the waveform toolpath

Regarding the pitting of the edges of the pockets, 3 sections can be distinguished in the toolpath of the waveform (Fig. 4.). In the first 5th pockets, the edges of the pockets are rarely 180-190 µm. From the 6th pocket, the size of the pitting shows an increase. Their average size ranged from 300 to 400 µm. This process can be observed up to the 20th pocket. From the 21st pocket, continuous crackling and cratering can be observed along the edge, with an average size of 600-1000µm.
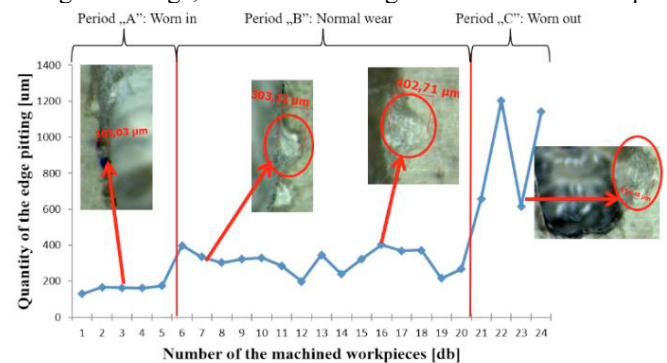

Figure 4. Changes in the cracking and chipping of the edges of manufactured pockets in the case of a waveform

At the trochoidal toolpath, material cracking was almost unchanged up to the first 15 pockets (180-200 µm) (Fig. 6). Up to the first 4 pockets, 1-2 such places were observed along the perimeter, however, from the 5th pocket, this phenomenon can be observed almost the entire length of the examined contour. Therefore, the end of the wear section was determined at pocket 4. At the 16th pocket, the onset of crater cracking was observed. From here, the size of the squares began to increase rapidly along the perimeter.
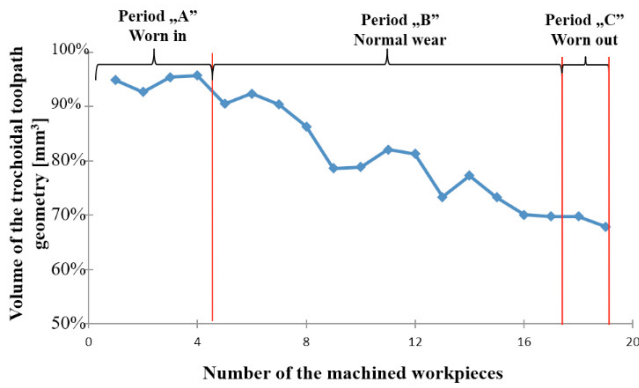
Figure 5. Changes in the volume of the machined pockets at the Trochoidal toolpath
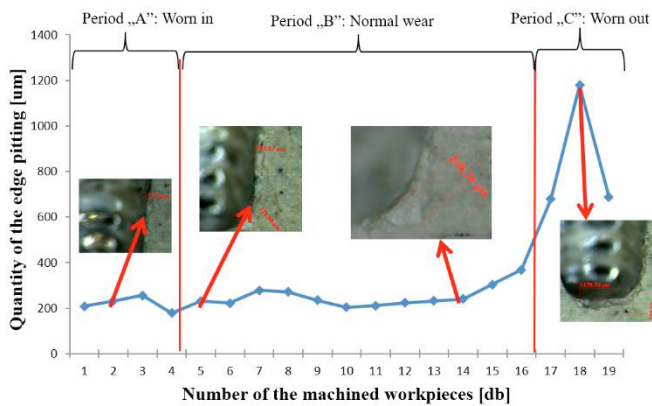

Figure 6. Changes in the cracking and chipping of the edges of manufactured pockets in the case of a trochoidal toolpath

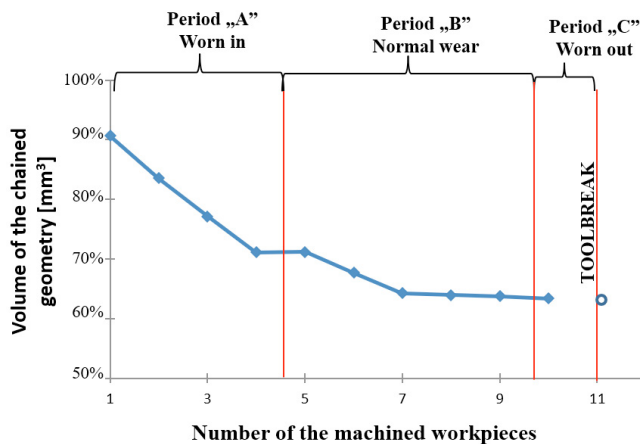Finally, the chained toolpath strategy was also analysed.

Figure7. Changes in the volume of the machined pockets at the Chained toolpath

On the chained toolpath, similarly to the other strategies, the average width of the chippings in the first section was between 180-200 μm (Fig. 8). However, unlike the others, they did not appear here scattered, but in context. The phenomenon was observed along a length of 1-1.5 mm. The first section up to pocket 4 was almost unchanged. From the 5 pockets, the width dimensions of the craters ranged from 280 to 300 μm. The final

phase followed from pocket 8, where crackles and crater wear were observed at almost the entire geometry produced.
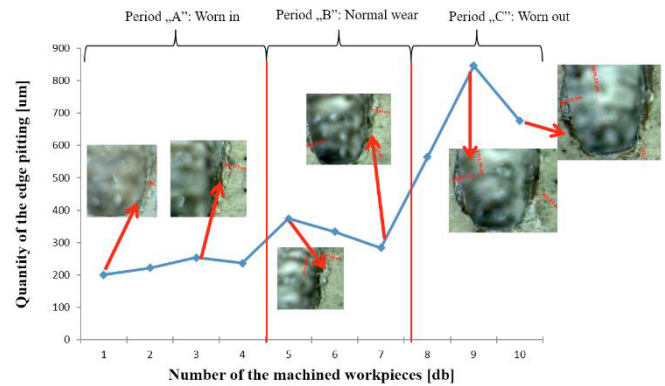

Figure 8. Changes in the cracking and chipping of the edges of manufactured pockets in the case of a chained toolpath

4. INVESTIGATION OF THE TOOL WEAR CONDITION

The analysis of the process of pocket edge pitting was followed by the evaluation of microscopic images of the tools taken at a given checkpoint (every 5th pocket) (Móricz et al. 2019). The direct analysis of the tool wear was important to get an idea of how consistent the tool wear is with the analyses documented in the previous sections, and to collect information on the complex wear of the tool edge geometry. The maximum of machined pockets was 24, but in some cases the tool broke much earlier.
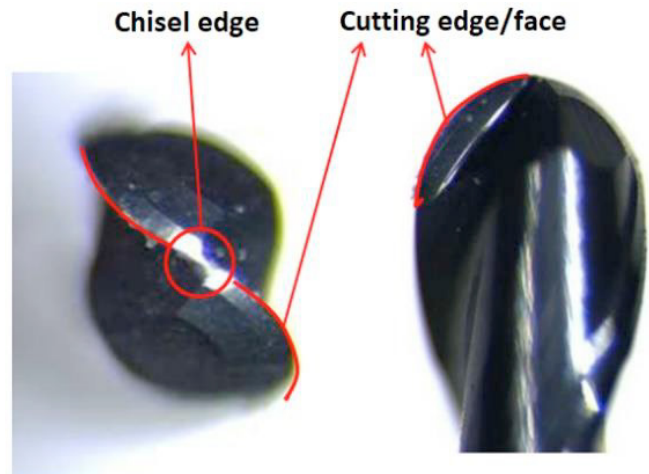

Figure 9. Most important wearing places at the early tool life period

During the measurement, a curve was fitted along the worn length of the cutting edge in the software used to determine the longitudinal wear of the edge, and the area of the face was also determined (Fig. 9). At each checkpoint, the tool could not be positioned in the same position in all cases, so the depth value of the wear could be deduced from the 3D model of the tool. Based on the 3D model of the tool and the microscopic images, it was determined that the tool deviates from the horizontal line by a maximum of 20°. A worn part with a diameter of 0.1 mm has been marked on the model. Using ICMEASURE (on-screen image measurement and image acquisition software), the diameter and area of the worn part were also determined.

Subsequently, the area of the worn part was also measured at a tool rotation of 20°. There is an 8-9% difference between the two areas, so this is the same error between each image when measuring microscopic images.
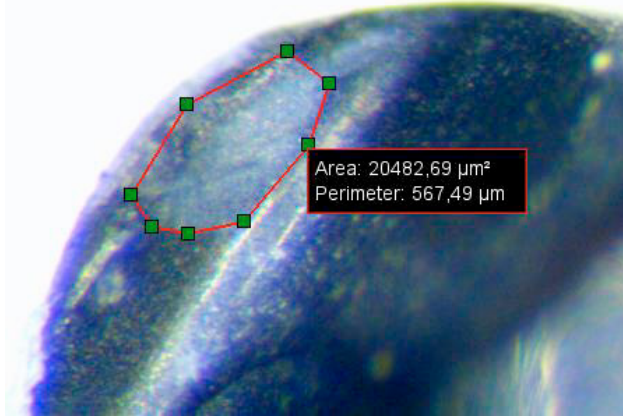

Figure 10. Measuring the area of a worn rake face from microscopic images of a tool

24 pockets were machined using the waveform toolpath. 6 control points were defined during the analysis. The first checkpoint belongs to the sharp tool. The second is right after the 5th pocket, the third point after 10th pocket, the fourth checkpoint after 15th pockets, and the fifth checkpoint after 20th pocket. During the analysis, tool wear could only be measured up to 20th pocket, as in 24th pocket, the cutting part of the tool was completely worn. Here, the total surface area of the tool face was determined during the calculation of the worn surface.
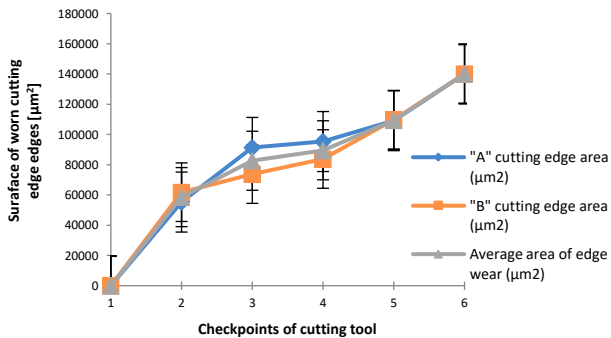

Figure 11. Phases of tool wear at the waveform toolpath

The corrected measurement values of wear are shown in Fig.11. A large jump is observed after machining 5th pocket compared to the sharp tool (checkpoint 2). Up to 15th pocket the wear rate decreased (check point 4), then from 20th pocket (check point 5) the tool was completely worn out (from 20th pocket the tool glowed was observed.)

The next tool analysed is the tool used in trochoidal machining. After the 5th pocket, in contrast to the waveform toolpath, a significant difference can be observed between the two edges (checkpoint 2). Thus, it can be said that up to the 5th pocket, rapid tool wear occurred in this case as well. Up to the 15th pocket, the wear rate of the "A" rake face decreased, while the "B" rake face showed a linear increase (checkpoint 4). In the last stage, the total wear of the tool showed a steady acceleration. From the 16th pocket, a glow of the tool was also observed.
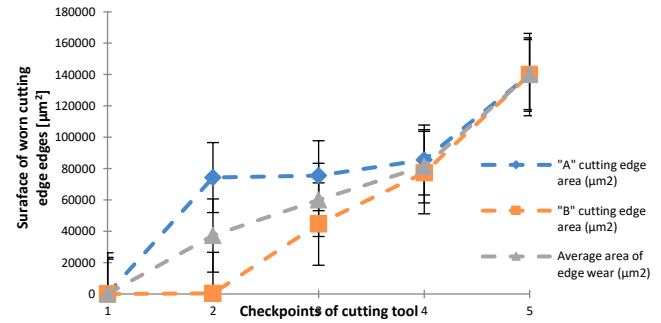

Figure 12. Tool wear phases at trochoidal toolpath

In the case of a chained toolpath, there is no significant difference between the wear processes of the two cutting edges. Unlike previous technologies, the wear on the cutting edges was much faster. There was a tool break in the 11th pocket.
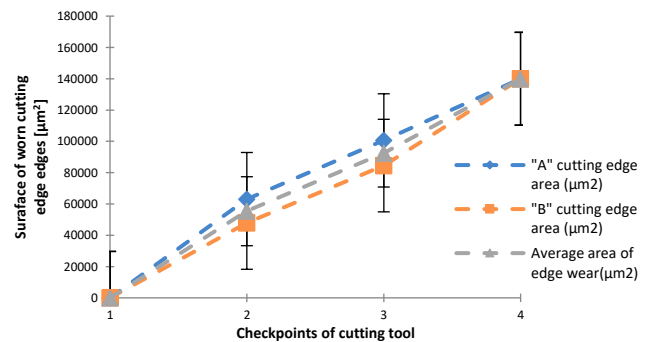

Figure 13. Tool wear phases at a chained toolpath

In the chained toolpath, a linear wear process can be observed based on the microscopic images of the tool.

5. CONCLUSIONS

The paper analysed the direct and indirect tool wearing for micro-milling of ceramics. Under ideal conditions chip removal takes place in the ductile range. Due to tool wearing, this contact surface changes, the cutting force begins to oscillate, and then the initial cracking and pitting of the machined surface can be observed. In the region of brittle chip removal, the oscillation of the cutting force continues increasing and coarse crater cracks appear on the surface. The aim of the research was to explore the relationship between the changes in the geometrical characteristics of the manufactured pockets, the wear conditions of the tool and the pitting phenomena on the edge of the machined workpiece. During the study, 3 toolpaths were analysed, which are the following: waveform, trochoidal toolpath, chained toolpath.

- Based on the evaluation of the data, it can be concluded that the *waveform* proved to be the best strategy among the examined toolpaths, as in this case most pockets could be manufactured. The wear phase of the Taylor curve ends at the 5th pocket based on both the volume change and the cracking. Microscopic analysis of the tool also showed this result.

- In the case of a *trochoidal* toolpath, the tool enters the linear wear phase at the 5th pocket based on the examination of the volume and the cracking. Based on

the examination of the tool, the wear rates of the two cutting edges differed significantly. While the cutting edge of "A" at the 6th pocket was already in the linear range (normal cutting), the cutting edge of "B" was still intact.

- In the case of a *chained* toolpath, these tool wearing stage changes are difficult to establish due to the small number of pockets produced (early break of the tool). Based on the geometric analysis of the manufactured pockets, it can be concluded that after the 4th pocket it enters the linear wear phase. However, due to the small number of elements in the tool analysis, tool wear in this case can no longer be clearly attributed to the geometric change of the pockets.

The curves obtained from the change in volume and the curves obtained based on the cracking and the measured data obtained during the analysis of tool wear overlap to a large extent, this is the main conclusion and result of the paper.

6. ACKNOWLEDGEMENT

REFERENCES

Bauernhansl, T., & Miehe, R. (2020). Industrielle Produktion–Historie, Treiber und Ausblick. Fabrikbetriebslehre, pp. 1-33). Springer Vieweg, Berlin, Heidelberg.

Blackley, W.S., Scattergood, R.O. (1991) Ductile-regime machining model for diamond turning of brittle materials. *Precision Engineering*, Volume (13), pp. 95-103. https://doi.org/10.1016/0141-6359(91)90500-I

Glawar, R., Ansari, F., Matyas, K. (2021). Evaluation of Economic Plausibility of Integrating Maintenance Strategies in Autonomous Production Control: A Case Study in Automotive Industry. *IFAC PapersOnLine,* pp. 43–48

Antwi, E. K., Liu, K., Wang, H. (2018.) A review on ductile mode cutting of brittle materials, *Frontiers of Mechanical Engineering*. Volume (13), No. 2, pp. 251–263, https://doi.org/10.1007/s11465-018-0504-z

Bifano, T., Dow, T., Scattergood, R. (1991) Ductile-regime grinding: a new technology for machining brittle materials, *Journal of Engineering for Industry*, Volume (113), pp.184-189.

Heleen, R., Eleonora, F., Jan, B., Dominiek, R., Bert, L. (2014.) Micromilling of sintered ZrO_2 ceramic via cBN and diamond coated tools. *Procedia CIRP*, Volume (14), pp. 371 – 376.

Kevin, F., Zhi, W., Takashi, M., Yong, H. (2009) Effect of tilt angle on cutting regime transition in glass micromilling. *International Journal of Machine Tools & Manufacture*, Volume (49), pp. 315–324.

Móricz, L., Viharos, Zs., Büki M., Szépligeti A. and Németh A. (2019). Product quality and cutting tool analysis for micro-milling of ceramics. *16th IMEKO TC10 Conference "Testing, Diagnostics & Inspection as a comprehensive value chain for Quality & Safety",* Berlin, Germany, ISBN: 978-92-990084-1-6, 95-100.

Móricz, L., Viharos, Zs., Büki M. (2020). Effect of CAM Path Strategies on Tool Life in Ceramics Micro-Cutting. *17th IMEKO TC 10 and EUROLAB Virtual Conference: "Global Trends in Testing, Diagnostics & Inspection for 2030"*, ISBN: 978-92-990084-6-1, pp. 92-98.

Móricz, L., Viharos, Zs., Büki, M., Szépligeti, A. and Németh, A. (2020). Off-line geometrical and microscopic & on-line vibration based cutting tool wear analysis for micro-milling of ceramics. *Measurement*, Volume (163), 18025. DOI:
https://doi.org/10.1016/j.measurement.2020.108025

Móricz, L., Viharos, Zs., Büki M. (2021). Vibration-based tool life monitoring for ceramics micro-cutting under various toolpath strategies. *ACTA IMEKO*, Volume (10), pp. 125–133.
https://doi.org/10.21014/acta_imeko.v10i3.1063

Móricz, L., Viharos, Zs. (2021). Vibration based characterization of tool wearing in micro-milling of ceramics. *Measurement: Sensors*, Volume (18), 100174

Muhammad, A., Mustafizur, R., Wong, Y. S. (2012). Analytical model to determine the critical conditions for the modes of material removal in the milling process of brittle material. *Journal of Materials Processing Technology*, Volume (212), pp. 1925-1933.

Muhammad, A., Zhang, X., Mustafizur, R., Senthi, L. (2013). A predictive model of the critical undeformed chip thickness for ductile–brittle transition in nano-machining of brittle materials. *International Journal of Machine Tools and Manufacture*, Volume (64), pp. 114-122.
10.1016/j.ijmachtools.2012.08.005

Rong, B., Eleonora, F., Jun, Q., Dominiek, R., Liang, L., Ning, H. (2012). Tool Wear Characters in Micro-milling of Fully Sintered ZrO_2 Ceramics by Diamond Coated End Mills. *Materials Science Forum*, Volume (723), pp. 365-370.https://doi.org/10.4028/www.scientific.net/MSF.723.365

Rong, B., Eleonora, F., Ning, H. (2013). Process investigation on meso-scale hard milling of ZrO2 by diamond coated tools. *Precision Engineering*, Volume (38), pp. 82-91. https://doi.org/10.1016/j.precisioneng.2013.07.007

Rong, B., Eleonora, F., Yinfei, Y., Jun, Q. (2018). Experimental Investigation on Ductile Mode Micro-Milling of ZrO_2 Ceramics with Diamond-Coated End Mills. *Micromachines*, pp. 127. https://doi.org/10.3390/mi9030127

Spath, D.; Westkämper, E.; Bullinger, H. J.; Warnecke, H. J. (2017). Neue Entwicklungen in der Unternehmensorganisation. Springer Berlin

Ueda, K., Sugita, T. and Hiraga, H. (1991). A J-integral Approach to Material Removal Mechanisms in Microcutting of Ceramics. *Annals of the CIRP*, Volume (40), pp. 61-64. https://doi.org/10.1016/S0007-8506(07)61934-9